Accuracy-precision trade-off in visual orientation constancy

M. De Vrijer
Donders Institute for Brain, Cognition and Behaviour, Radboud University Nijmegen, Nijmegen, The Netherlands

W. P. Medendorp
Donders Institute for Brain, Cognition and Behaviour, Radboud University Nijmegen, Nijmegen, The Netherlands

J. A. M. Van Gisbergen
Donders Institute for Brain, Cognition and Behaviour, Radboud University Nijmegen, Nijmegen, The Netherlands

Using the subjective visual vertical task (SVV), previous investigations on the maintenance of visual orientation constancy during lateral tilt have found two opposite bias effects in different tilt ranges. The SVV typically shows accurate performance near upright but severe undercompensation at tilts beyond 60 deg (A-effect), frequently with slight overcompensation responses (E-effect) in between. Here we investigate whether a Bayesian spatial-perception model can account for this error pattern. The model interprets A- and E-effects as the drawback of a computational strategy, geared at maintaining visual stability with optimal precision at small tilt angles. In this study, we test whether these systematic errors can be seen as the consequence of a precision-accuracy trade-off when combining a veridical but noisy signal about eye orientation in space with the visual signal. To do so, we used a psychometric approach to assess both precision and accuracy of the SVV in eight subjects laterally tilted at 9 different tilt angles (−120° to 120°). Results show that SVV accuracy and precision worsened with tilt angle, according to a pattern that could be fitted quite adequately by the Bayesian model. We conclude that spatial vision essentially follows the rules of Bayes' optimal observer theory.

Keywords: spatial vision, Bayesian modeling, vestibular, spatial constancy, psychophysics

Citation: De Vrijer, M., Medendorp, W. P., & Van Gisbergen, J. A. M. (2009). Accuracy-precision trade-off in visual orientation constancy. *Journal of Vision, 9*(2):9, 1–15, http://journalofvision.org/9/2/9/, doi:10.1167/9.2.9.

Introduction

Spatial awareness involves knowledge about body position in space and the ability to maintain a stable mental representation of space despite changes in body position. One way to assess spatial constancy is to test which line orientation is perceived as earth-vertical when the subject is roll-tilted in the absence of panoramic cues (subjective visual vertical, SVV). Numerous studies have shown that this task is subject to systematic errors (see Figure 1): Near upright, SVV errors are typically small (Figure 1A) but responses at intermediate tilts may show a shift away from head tilt (Figure 1B, E-effect; Müller, 1916) which has been linked to incomplete compensation for eye torsion (Curthoys, 1996; de Graaf, Bekkering, Erasmus, & Bles, 1992). Furthermore, it has been shown that the SVV becomes quite inaccurate at roll tilts beyond 60°, where it is biased toward head tilt (Aubert, 1861; Dyde, Jenkin, & Harris, 2006; Mittelstaedt, 1983; Schöne, 1964; Udo de Haes, 1970; Van Beuzekom & Van Gisbergen, 2000). These errors, also known as the Aubert- or A-effect (see Figure 1C), can be very substantial, sometimes reaching values up to 50° at head tilts near 120° (De Vrijer, Medendorp, & Van Gisbergen, 2008). In this study, our objective is to test whether the accuracy and precision characteristics[1] of the SVV are compatible with optimal observer theory.

Which computations must the brain perform in order to maintain visual orientation constancy? As shown in Figure 2, to estimate the visual vertical with respect to earth coordinates, the observer must combine information about line orientation on the retina with central signals compensating for the effects of head tilt and eye torsion. If these compensations are only partial, this will give rise to A- and E-effects, respectively. Accordingly, a simple explanation of the A-effect to be considered first is the possibility that the head tilt sensors systematically underestimate head tilt at large deviations from upright. However, several studies cast doubt on this explanation by showing that the perception of body tilt lacks the large inaccuracies of the SVV. Hence, this finding implies that the brain has access to a relatively accurate tilt signal (Kaptein & Van Gisbergen, 2004;

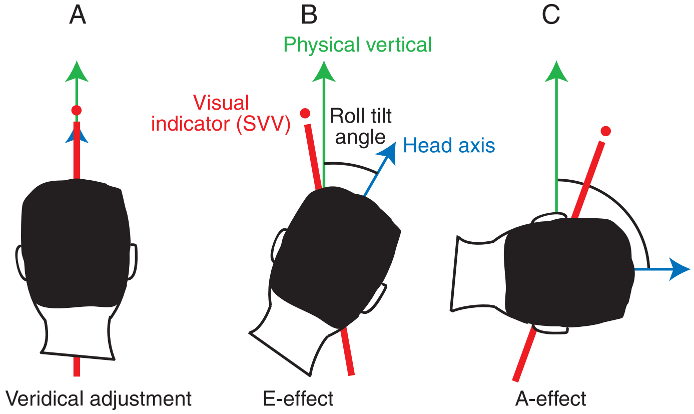

Figure 1. Schematic representation of bias patterns in SVV task. (A) Veridical adjustment at zero tilt. (B) E-effect (tilt overcompensation) may occur at intermediate tilt angles. (C) A-effect (tilt undercompensation) at larger tilt. Note that over- and under-*compensation* errors in the SVV are merely a description of the direction of the errors and need not imply that observers in fact over- or under*estimated* their tilt angle.

Mast & Jarchow, 1996; Mittelstaedt, 1983; Van Beuzekom, Medendorp, & Van Gisbergen, 2001) but does not use this signal as such in the computations underlying visual orientation constancy. Here we present the hypothesis that A- and E-effects reflect the results of a computational strategy, based on Bayesian observer theory, which aims to increase the precision of the compensatory signals near upright at the expense of reduced accuracy at larger tilt angles (De Vrijer et al., 2008; Eggert, 1998; MacNeilage, Banks, Berger, & Bülthoff, 2007). The general idea behind this theory is that the observer combines noisy sensory information about actual head tilt in space and eye rotation in the head, with prior knowledge about which tilt angle is most likely on an *a priori* basis.

As shown in Figure 2, optimal compensation, necessary to preserve orientation constancy despite head tilt, requires that the retinal line orientation ($\tilde{L}_E$) be compensated by a neural signal ($\tilde{E}_S$) that equals the actual eye orientation in space (E_S). Thus, to obtain a proper compensatory signal, the observer must take account of both the orientation of the head in space (H_S) and the orientation of the eye within the head (E_H). If the corresponding central estimates ($\tilde{E}_H$ and $\tilde{H}_S$) were veridical and precise, the observer would obtain an unbiased and stable percept of line orientation in space ($\tilde{L}_S$). However, if $\tilde{H}_S$ underestimates H_S, this would result in underestimation of eye-in-space angle E_S, thus causing an A-effect. By contrast, underestimation of ocular torsion would give rise to overestimating E_S, which would cause an E-effect. We now proceed to explain how such biases in $\tilde{H}_S$ and $\tilde{E}_H$ may be the downside of a noise-coping strategy in handling the raw neural signals from which they are derived ($\hat{H}_S$ and $\hat{E}_S$), even though the latter are assumed to be accurate, on average.

As proposed in Figure 2, the observer interprets the noisy eye-torsion and head-tilt signals by relying on a statistical approach. Their uncertainty is reflected in the width of corresponding likelihood functions that represent the range of potential underlying physical signals (indicated by orange sectors). Additionally, the Bayesian framework uses *a priori* knowledge about head tilt and ocular torsion, expressed in the prior probability distributions, which represent the fact that head tilt and eye torsion are mostly small. To combine the likelihood function and prior distribution optimally, the observer relies on their product, called the posterior distribution. When the subject is tilted, the posterior peaks in-between the peaks of the prior and the likelihood, thus giving rise to systematic errors: both head tilt and ocular torsion are systematically underestimated. However, the posterior distributions are less affected by sensory noise than the likelihood functions, thus yielding a precision that exceeds the precision of the sensory signals (see width of orange sectors). Hence, using prior knowledge affects the head-in-space and eye-in-head tilt estimates in two ways: it biases estimates toward smaller angles (reduced accuracy) but brings down uncertainty caused by sensory noise (increased precision). This strategy, an accuracy-precision trade-off, is particularly useful for small tilt angles, which are most common in daily life. For a full mathematical treatment of the scheme in Figure 2, see Methods section Modeling.

In a previous study (De Vrijer et al., 2008), we found that this computational strategy could account for the nonlinear increase of SVV errors with head tilt, if we made the assumption that the precision of the sensory head tilt signal decreases with tilt angle, as indicated by the noise increase in Figure 2 (bottom square panel). The purpose of the present study was to collect an extensive data set that would allow a thorough test of the Bayesian model. By testing eight subjects in a psychometric SVV experiment, we obtained estimates of SVV accuracy and precision at a range of tilt angles. Our results are consistent with the predictions of the Bayesian observer model, indicating that subjects use an optimal strategy to maintain visual orientation constancy.

Methods

Subjects

We tested eight subjects (5 male, 3 female), including the three authors who where familiar with the purposes of the experiment. Subjects, aged between 22 and 64 years (mean ±*SD*: 31 ± 14 yrs.), provided written informed consent to participate in the experiments. Participants were free of known vestibular or other neurological disorders and had normal or corrected-to-normal visual acuity.

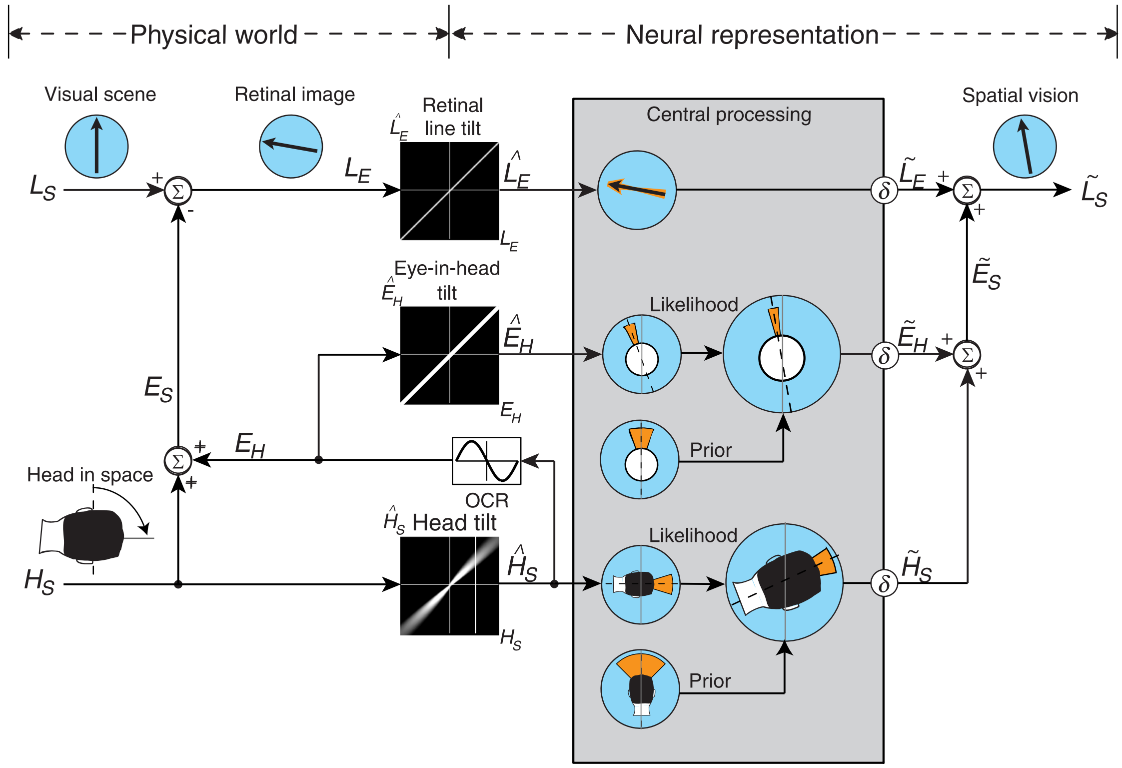

Figure 2. Neural compensation for head tilt and eye torsion to maintain visual orientation constancy. The purpose of the scheme is to elucidate the relations between physical variables and internal signals engaged in visual spatial perception. A world-vertical line (line-in-space, $L_S = 0$) appears in front of a tilted observer (head-in-space, $H_S = 90°$). Head rotation and ocular counterroll (OCR, eye-in-head E_H) result in net retinal image tilt (line-on-eye, L_E) according to: $L_E = L_S - (H_S + E_H)$. Signal $\hat{H}_S$, coding head orientation in space, is assumed to be accurate but contaminated by Gaussian noise with an amplitude that increases linearly with tilt angle (bottom square panel; gray levels encode probability). Likewise, signal $\hat{E}_H$, encoding eye orientation in the head, is accurate but contaminated by independent Gaussian noise. Ideal observer uses Bayesian strategy to obtain an optimal estimate of head in space ($\tilde{H}_S$) and eye in head ($\tilde{E}_H$) to reconstruct eye orientation in space ($\tilde{E}_S$). The latter signal is then combined with retinal signal ($\tilde{L}_E$) to obtain an internal estimate of the orientation of the line with respect to gravity ($\tilde{L}_S$). Orange sectors in the Bayesian scheme symbolize the widths of the sensory and prior distributions. Decision rule (δ) picks angle with maximum *a posteriori* probability (MAP). Note that biased estimates of $\tilde{E}_H$ and $\tilde{H}_S$ have opposite biasing effects on the perceived line orientation in space and that $\tilde{L}_S$ in the illustrated example is not veridical so that a world-vertical line does not appear upright to the tilted observer. If the observer, in this particular example, was to adjust the line to the subjective vertical (SVV), it would be rotated in clockwise direction, which amounts to an A-effect as illustrated in Figure 1. If the error in $\tilde{E}_H$ were larger than in $\tilde{H}_S$, this would result in an opposite effect, with the perceived line oriented clockwise of vertical (E-effect).

Setup

Subjects were seated in a computer-controlled vestibular chair with nested gimbals, which was configured to allow subject rotation in roll. The subject's trunk was tightly fixed using adjustable shoulder and hip supports and a five-point seat belt. The legs and feet were restrained with Velcro straps and the head was firmly fixed in a natural upright position for looking straight ahead, using a padded helmet. For each subject, seat adjustments ensured that the roll-axis of the chair coincided with the naso-occipital axis midway between the eyes. Tilt position was measured using a digital position encoder with an angular resolution of 0.04°. A luminous line, consisting of a roughened glass fiber, lit by a white LED, was mounted in front of the subject at a distance of ~90 cm, so it had an angular subtense of 20°. The rotation axis of the line coincided with the chair rotation axis and its orientation was computer-controlled with an angular resolution of 0.5°. A bright dot at one end served for polarization (see Figure 1). Subjects were free to move their eyes in any direction and vision was always binocular. Except for the luminous line, experiments were performed in complete darkness.

Experimental paradigm

The experiment was designed to obtain psychometric curves about subjective visual verticality at 9 roll tilt angles, ranging from −120 to 120° in 30°-intervals, which were tested in random order. Each experimental run started with the subject in upright position. Then, the lights were turned off and subjects were rotated to a tilt angle H_S in total darkness, with right-ear-down angles coded as positive. Rotation was performed at a constant angular velocity of 30°/s, which was reached within 1s using a peak acceleration of 50°/s^2. After a 30-s waiting period that allowed canal effects to subside, subjects viewed the polarized luminous line with the appearance of an inverted exclamation mark (see Figure 1) for a brief period of 20 ms and indicated whether its orientation in space was clockwise (CW) or counterclockwise (CCW) from their perceived direction of gravity, using a toggle switch. Subsequently, a new trial followed with a different line orientation, picked randomly from a set of 11 line orientations (details follow below). This sequence was repeated until all line orientations had been tested, after which subjects were rotated back to upright and lights were turned on, during a 30s resting period. Positive and negative body tilt angles were alternated regularly. For the 0°-tilt condition, we added an equal number of catch trials, in which subjects were tilted to an angle that was picked randomly from the range of ±5°, using a sub-threshold rotation speed of 2°/s, so that they could not perform the task in body coordinates.

To collect psychometric data we used the method of constant stimuli (Ehrenstein & Ehrenstein, 1999). The set of 11 line orientations was centered on a coarse estimate of the SVV threshold at each tilt angle, which was determined with the method of adjustment in a preceding session. For all tilt angles except for upright ($H_S = 0°$), test orientations were presented at 0, ±3, ±6, ±9, ±12, and ±15° relative to this value. For upright, where performance was typically more precise, we used a narrower test range at 0, ±2, ±4, ±6, ±8, ±10°. Each set of line orientations was presented in 12 experimental runs in random order, yielding a total of 132 responses for each psychometric curve. For each subject, data were collected in a total of 5 sessions of approximately 45 min. each. Catch trial responses were excluded from further analysis.

Data analysis

We quantified behavioral performance by measuring the proportion of CW responses as a function of line orientation. Psychometric data were quantified by fitting with a cumulative Gaussian function:

$$P(x) = \lambda + (1 - 2\lambda)\frac{1}{\sigma\sqrt{2\pi}}\int_{-\infty}^{x} e^{-(y-\mu)^2/2\sigma^2}dy \qquad (1)$$

in which x represents line orientation. The mean of the Gaussian, μ, represents the subjective vertical in the SVV task. The width of the curve, σ, serves as a measure for the subject's uncertainty in the SVV and is inversely related to precision. Parameter λ, representing the lapse rate, accounts for stimulus-independent errors caused by subject lapses or mistakes, and was restricted to small values ($\lambda < 0.06$). Fits were performed using Matlab 7.0 software (The MathWorks) with the routine "psignifit" (Wichmann & Hill, 2001b).

Modeling

We first provide a short step-by-step description of the Bayesian observer model, which extends an earlier version (De Vrijer et al., 2008) by including an optimal-observer interpretation of the E-effect. The model, schematically illustrated in Figure 2, uses the following conventions: physical variables are denoted by a capital with a subscript denoting the reference frame. For example, E_H represents the (physical) roll orientation of the eye (E) with respect to the head (H). Sensory signals are denoted by a *hat* symbol (ˆ), as in $\hat{E}_H$, reflecting the orientation of the eye in the head as measured by the sensors. The outcome of a Bayesian computation is denoted by a *tilde* symbol (~), as in $\tilde{E}_H$, which represents the optimal estimate of eye-in-head orientation according to sensory information and prior knowledge.

Head-in-space estimation

In the model, we assume that the sensory head tilt signal ($\hat{H}_S$), measured by a variety of tilt sensors, is a noisy but unbiased representation of the physical head tilt angle (H_S). Thus, the sensory tilt signal varies in repeated trials at the same physical tilt angle but the expected value of $\hat{H}_S$ is a veridical representation of the actual head tilt. Conversely, this means that the brain cannot be sure about the physical angle, based on the sensory signal, and needs a statistical approach to determine the best estimate of head tilt angle. The Bayesian model assumes that the brain is adapted to the noise properties of its sensors, which allows it to deduce the probability of each tilt angle based on the sensory evidence, known as the likelihood function $P(\hat{H}_S|H_S)$. When sensory noise increases, the likelihood function, which is modeled by a Gaussian centered on $\hat{H}_S$ and with standard deviation $\sigma_{\hat{H}_S}$, becomes less peaked and broader. To account for the typical nonlinear increase of the A-effect with tilt, the model allows for the possibility that the precision of the tilt sensors decreases with tilt angle, like in De Vrijer et al. (2008). This is formulated by stating that noise in the sensory head-tilt signal ($\sigma_{\hat{H}_S}$) increases rectilinearly with tilt angle according to:

$$\sigma_{\hat{H}_S} = a_0 + a_1|H_S| \qquad (2)$$

in which a_0 reflects the noise at $H_S = 0°$ and a_1 represents the proportional increase of noise with tilt angle (see square bottom panel in Figure 2). Note, however, that by setting the lower limit of parameter a_1 to zero, the model did not force tilt-sensor precision to be dependent on head tilt.

To obtain an optimal estimate of the physical tilt position, the brain further takes into account that some tilt angles are more likely on an *a priori* basis. In the model, this is expressed by the prior distribution $P(H_S)$, which is modeled by a Gaussian with standard deviation σ_{H_S}, centered on zero head tilt ($H_S = 0°$), reflecting the knowledge that small head tilts are more likely than large tilts. Multiplication of the likelihood and prior distributions yields the posterior probability distribution $P(H_S|\hat{H}_S)$ according to Bayes' rule: $P(H_S|\hat{H}_S) = k \cdot P(\hat{H}_S|H_S) \cdot P(H_S)$, in which k serves a normalization purpose. The peak of the posterior probability function is in-between the peaks of the likelihood and prior distributions, depending on their relative widths (Carandini, 2006; Knill & Pouget, 2004; MacNeilage et al., 2007). In the model, the peak of the posterior ($\tilde{H}_S$) is used as the optimal estimate of head tilt angle.

Eye-in-head estimation

Since the eyes typically counterroll in their orbits during roll tilt (de Graaf et al., 1992; Markham & Diamond, 2002; Palla, Bockisch, Bergamin, & Straumann, 2006), an ideal observer also needs an estimate ($\tilde{E}_H$) of the actual torsional orientation of the eyes with respect to the head, E_H (see Figure 2). Following Palla et al. (2006) we approximated eye-torsion by: $E_H = -A \cdot \sin(\hat{H}_S)$, in which A represents the maximum torsion amplitude and $\hat{H}_S$ reflects the sensory head-tilt signal. The negative sign reflects the fact that the eyes counterrotate relative to the head. Information about torsional eye-in-head orientation ($\hat{E}_H$), whether based on an efference copy signal, or on proprioception, or both, is treated as a sensory signal, assumed to be accurate but contaminated by noise ($\sigma_{\hat{E}_H}$). It is important to note that this noise is introduced by the systems monitoring the torsion signal and has nothing to do with noisy variations in the torsion signal itself, hence is assumed to be independent of $\sigma_{\hat{H}_S}$. We assumed that the observer again uses a Bayesian strategy to obtain an optimal estimate of eye-in-head orientation ($\tilde{E}_H$), by taking into account which orientations are most likely on an *a priori* basis. Here, prior knowledge entails that the eyes are mostly closely aligned with the head (i.e. $E_H \sim 0°$). Sensory information about torsional eye position is represented by the likelihood function $P(\hat{E}_H|E_H)$ and prior knowledge is represented by a Gaussian centered on 0° with standard deviation σ_{E_H}. The peak of the posterior distribution is used as the optimal estimate of eye-in-head angle ($\tilde{E}_H$).

Accuracy and precision predictions of complete model

The estimates of eye-in-head ($\tilde{E}_H$) and head-in-space ($\tilde{H}_S$) are combined to obtain an optimal estimate of the orientation of the eye in space ($\tilde{E}_S$), which is then used as the compensating signal in the SVV task. The expected value of $\tilde{E}_S$ in many repeated trials ($\mu_{\tilde{E}_S}$) follows from the corresponding expected values of $\tilde{H}_S$ and $\tilde{E}_H$. As shown in Appendix A, this results in the following relation:

$$\mu_{\tilde{E}_S} = \mu_{\tilde{H}_S} + \mu_{\tilde{E}_H} = \frac{\sigma^2_{H_S}}{\sigma^2_{H_S} + \sigma^2_{\hat{H}_S}} \cdot H_S + \frac{\sigma^2_{E_H}}{\sigma^2_{E_H} + \sigma^2_{\hat{E}_H}} \cdot E_H \quad (3)$$

This relation specifies how prior knowledge and sensory uncertainty bias the eye-in-space estimate. Note that noise in the sensory signals causes an underestimation of head-in-space and eye-in-head. Furthermore, the tilt dependency of $\sigma_{\hat{H}_S}$ (Equation 2) causes a slight skewness in the head-tilt likelihood function, which was neglected to enable a straightforward fitting procedure.

The variance in the maxima of the posteriors (MAP) in repeated trials is smaller than the variance of the posteriors themselves (see Appendix A). As a result, the variance in $\tilde{E}_S$ in repeated trials ($\sigma^2_{\tilde{E}_S}$) is given by:

$$\sigma^2_{\tilde{E}_S} = \sigma^2_{\tilde{H}_S} + \sigma^2_{\tilde{E}_H} = \left(\frac{\sigma^2_{H_S}}{\sigma^2_{H_S} + \sigma^2_{\hat{H}_S}} \cdot \sigma_{\hat{H}_S}\right)^2 + \left(\frac{\sigma^2_{E_H}}{\sigma^2_{E_H} + \sigma^2_{\hat{E}_H}} \cdot \sigma_{\hat{E}_H}\right)^2 \quad (4)$$

which shows that prior knowledge reduces uncertainty caused by sensory noise. Equations 3 and 4 provide insight into the structure of the model from a forward perspective. However, attempting to fit all its parameters would confront us with an underdetermined inverse problem. This problem can only be solved by making a few simplifying assumptions which will be detailed in the next subsection where we summarize the fit parameters that were actually determined.

Fit parameters of simplified model

SVV accuracy

To obtain an estimate of the world-centered orientation of the line ($\tilde{L}_S$), required in the SVV task, the central estimate of eye position in space $\tilde{E}_S$ is added to the estimated retinal line orientation $\tilde{L}_E$, which is assumed to be unbiased ($\tilde{L}_S = \tilde{L}_E + \tilde{E}_S$). Thus, according to the model, the systematic errors in the SVV (μ_{SVV}) are caused exclusively by bias in the eye-in-space estimate, as shown in the following relation:

$$\mu_{\mathrm{SVV}} = E_S - \mu_{\tilde{E}_S} = \left(H_S - \mu_{\tilde{H}_S}\right) + \left(E_H - \mu_{\tilde{E}_H}\right) = \frac{\sigma^2_{\hat{H}_S}}{\sigma^2_{H_S} + \sigma^2_{\hat{H}_S}} \cdot H_S - \frac{\sigma^2_{\hat{E}_H}}{\sigma^2_{E_H} + \sigma^2_{\hat{E}_H}} \cdot A\sin(H_S) \quad (5)$$

Here, the first term on the right-hand side represents the error in the head-in-space estimate, which contributes to the A-effect, whereas the second term reflects the error in the eye-in-head estimate and contributes to the E-effect. Note that fitting the first term actually involves 3 parameters: the tilt noise parameters a_0 and a_1 (see Equation 2) and the head prior, σ_{H_S}. Complete fitting of the second term would also involve 3 parameters (A, σ_{E_H} and $\sigma_{\hat{E}_H}$). To prevent problems of overfitting, we simplified the second term to a single parameter (ΔE_H), representing the uncompensated magnitude of eye torsion based on the following consideration: If we assume that both the noise in the central estimate of eye torsion ($\sigma_{\hat{E}_H}$) and the width of the torsion prior (σ_{E_H}) are constant (i.e. independent of H_S), the second term on the right-hand side of Equation 2 reduces to a scaled version of the actual eye torsion E_H. In other words, uncompensated torsion is a scaled version of the actual torsion, with the same sinusoidal tilt relation:

$$\frac{\sigma^2_{\hat{E}_H}}{\sigma^2_{E_H}+\sigma^2_{\hat{E}_H}}\cdot A\sin(H_S)=\frac{1}{r^2+1}A\cdot\sin(H_S)$$
$$=\Delta E_H\sin(H_S)\ \text{with}\ 0\le\Delta E_H\le A \tag{6}$$

Here ΔE_H represents the uncompensated part of the eye-in-head amplitude (A) and r^2 reflects the ratio of the variances of the eye-torsion prior and sensory eye-in-head signal ($\sigma^2_{E_H}/\sigma^2_{\hat{E}_H}$). Thus, the narrower the prior relative to the torsion noise distribution, the larger the uncompensated torsion ΔE_H.

SVV precision

SVV scatter (σ_{SVV}) is determined by a combination of head-in-space noise ($\sigma_{\tilde{H}_S}$), which is assumed to be tilt dependent (see Equation 2) and two tilt-independent terms, viz. eye-in-head noise ($\sigma_{\tilde{E}_H}$) and retinal noise ($\sigma_{\tilde{L}_E}$). However, to prevent problems of overfitting, the contributions of the latter two terms were not fitted separately. This means that both tilt-independent noise terms were attributed to the first term in Equation 4. Effectively, the simplified model fitted SVV variability with 3 parameters (a_0, a_1 and σ_{H_S}), using:

$$\sigma^2_{SVV}\approx\sigma^2_{\tilde{E}_S}\approx\sigma^2_{\tilde{H}_S}=\left(\frac{\sigma^2_{H_S}}{\sigma^2_{H_S}+\sigma^2_{\hat{H}_S}}\cdot\sigma_{\hat{H}_S}\right)^2 \tag{7}$$

Because of this simplification, both $\sigma_{\hat{H}_S}$ and σ_{H_S} were somewhat overestimated, but, as we discuss later (see section Effect of simplifying assumptions in Discussion) the effect is probably minor and does not affect our overall conclusion. Note that the impact of eye-in-head noise on the accuracy of the eye-in-space estimate (Equation 3) was taken into account.

Parameter	Definition	Equation
a_0 [°]	Noise in sensory head-tilt signal ($\sigma_{\hat{H}_s}$) at 0° head tilt	2
a_1 [°/°]	Increase of noise in sensory head-tilt signal ($\sigma_{\hat{H}_s}$) with tilt angle	2
σ_{H_s} [°]	Width of head-tilt prior distribution	3 and 4
ΔE_H [°]	Maximum amplitude of uncompensated ocular counterroll	6

Table 1. Summary of fit parameters.

In summary, the simplified model has four fit parameters, (a_0, a_1, σ_{Hs}, and ΔE_H) that determine the accuracy and the precision of the SVV at each head tilt angle (see Table 1).

Model fits

The Bayesian model makes simultaneous predictions of systematic SVV errors (μ_{SVV}) and SVV variability (σ_{SVV}) as a function of head tilt angle H_S. We used a maximum-likelihood estimation (MLE) procedure to fit the model to the psychophysical responses. We obtained the best-fit values of the four parameters for each subject by minimizing the negative log-likelihood using the fmincon routine (Matlab 7.0; The MathWorks). The log-likelihood function $L(\theta)$ is defined as $L(\theta)=\sum_{i=1}^{n}\log(P_\theta[N_i(CW)\,|\,\theta])$, in which $P_\theta[N_i(CW)\,|\,\theta]$ represents the chance of obtaining $N_i(CW)$, the number of 'CW'-responses at a particular combination of head tilt and line orientation, for a given parameter set θ. $P_\theta[N_i(CW)\,|\,\theta]$ was computed by first calculating μ_{SVV} and σ_{SVV} at each tilt angle for a given parameter set, using Equations 5 and 7. The chance of obtaining a 'CW'-response ($P[CW]$) at a certain combination of tilt angle and line orientation was calculated using the normal cumulative distribution function. Moreover, since subjects may have made stimulus-independent lapses, we included a lapse rate (λ) into the distribution function. For simplicity, the lapse rate in these model fits was set at a fixed value of 0.06 (Wichmann & Hill, 2001a). Subsequently, the chance of obtaining N_i 'CW'-responses (given 12 repetitions) was specified by the binomial distribution, B(12, $P[CW]$).

Standard deviations of the best-fit parameters (see Table 2) were obtained by performing 100 bootstraps.

Results

To test the predictions of the extended Bayesian observer model, we investigated the sense of visual verticality (SVV) in roll-tilted subjects, using a psychometric approach. We start this section with a description of the data, followed by the model fit results.

Psychometric SVV results

To obtain a quantitative assessment of the accuracy and precision of the SVV, subjects performed a psychophysical task (forced-choice), in which they judged the orientations of a set of luminous lines with respect to gravity. Figure 3 illustrates how roll tilt (H_S) affected the SVV of a typical subject (RV). Each panel shows how the proportion of '*CW*' responses, $P(CW)$, changed as line orientation in space was varied around perceived vertical. At each tilt angle, response rates range from 0 to 1, indicating that the stimulus sets were positioned correctly. In an ideal observer, all psychometric functions would resemble a step centered at zero. In fact, as body tilt increases, psychometric curves shift away from zero and become less steep as a sign that there is decay in both accuracy and precision. For example, an earth-vertical line

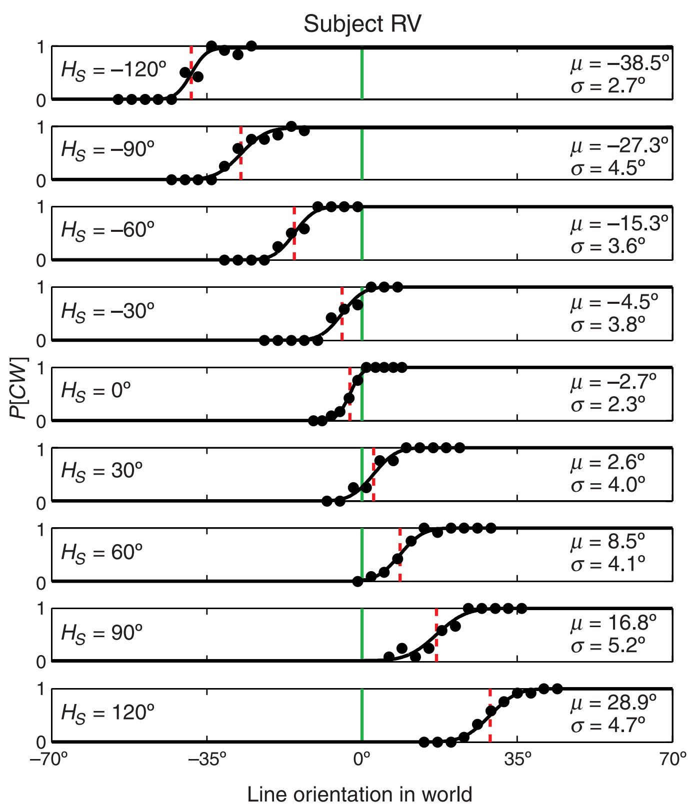

Figure 3. Psychometric SVV data, with each panel representing a different head tilt angle H_S. Proportion of "*CW*" responses is plotted against line orientation with respect to gravity. Solid line: best-fit cumulative Gaussian, characterized by μ and σ. Vertical dashed lines denote μ, a measure for SVV accuracy. Verticality perception is less accurate (curves are shifted with respect to 0°) and less precise (curves are less steep) as head tilt increases. Subject: RV.

(0°) is always perceived as "*CW* from earth vertical" at −60° head tilt, whereas it is always perceived as "*CCW* from vertical" at 60° head tilt. For each tilt angle, we fitted the data with a cumulative Gaussian function (see Equation 1), which is characterized by three parameters: mean (μ), *SD* (σ) and lapse rate (λ). We took μ as a measure for accuracy and used $1/\sigma^2$ as a measure for the precision of the verticality percept. When precision improves, σ becomes smaller and hence the psychometric curve becomes steeper.

In the upright body position (H_S = 0°), the percept of visual verticality is virtually unbiased and relatively precise compared to the other tested tilt angles. In the top panel (H_S = −120°), the mean of the psychometric curve is at μ = −38.2°, which means that the line must be tilted away from true vertical by this angle to be perceived as vertical in space, an expression of the A-effect (Aubert, 1861). In the bottom panel (H_S = +120°), the curve is centered at μ = +28.7°, which again reflects an A-effect. To appreciate the deterioration in precision, notice that the curve is steepest at 0° roll tilt (σ = 2.3°) and that σ increases at larger tilt angles, reaching maximum values of 5.8° and 5.1° at H_S = +90° and H_S = −90°, respectively.

Figure 4 shows best-fit μ-values from all subjects to illustrate how the accuracy of the verticality percept changes as a function of tilt angle. Model fits through the data will be discussed below (see section Model fit results). With one notable exception (DB), all subjects show variations of the response pattern known from the literature (De Vrijer et al., 2008; Mittelstaedt, 1983; Udo de Haes, 1970; Van Beuzekom et al., 2001; Van Beuzekom & Van Gisbergen, 2000), with less consistent systematic errors at small tilts and gradually decreasing accuracy, in the form of increasing A-effects, at larger tilt angles. Furthermore, several subjects show E-effects at the intermediate tilt angles, ranging up to −13.2° at 60° roll tilt for subject FW.

To show how tilt affects SVV precision, Figure 5 plots parameter σ of the fitted psychometric curves as a function of tilt angle for all subjects. Again, model fits will be discussed in the section Model fit results. Invariably, precision is best at 0° tilt and deteriorates with tilt angle (one-way ANOVA; $F(8,63) = 5.3$, $P < 0.001$). Values for σ range from ~2° at zero tilt to a maximum of about 7° (PM) at the largest roll tilt angles. These findings are consistent with anecdotal reports from several subjects that judging the visual vertical was more difficult at the largest tilt angles.

The deterioration in SVV accuracy and precision with tilt angle is also manifest in the data pooled across subjects. As Figure 6A shows, the population mean has a clear A-effect at the larger tilt angles, as a sign of decreased accuracy. The E-effect, which was observed in several subjects at smaller tilts (≤60°), is negligibly small at the population level. The decay in precision with tilt angle shown by present results is depicted in Figure 6B. As shown, σ steeply increases between 0° and ±30° tilt

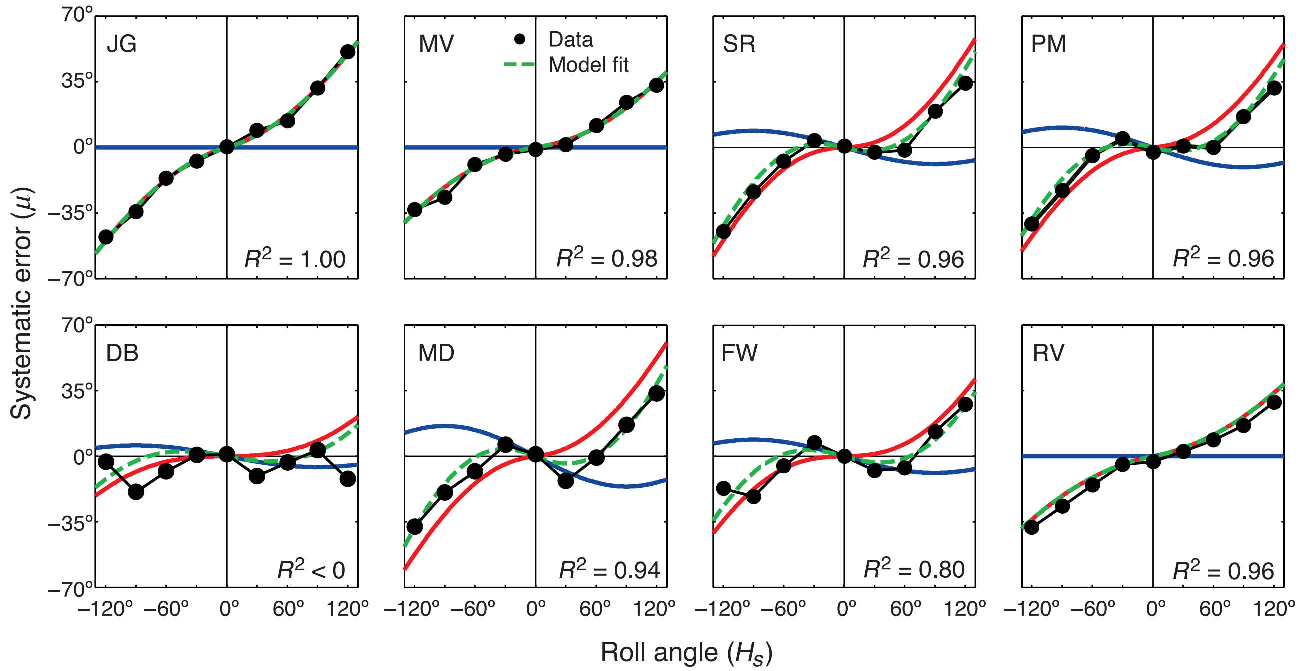

Figure 4. Accuracy of the SVV plotted against head tilt angle for all subjects. Filled circles: Systematic errors, based on μ-values from psychometric functions (see Figure 3). Dashed line: Bayesian model fit. Red line: error contribution due to underestimation of head angle. Blue line: error contribution due to underestimation of eye torsion. R^2-values represent goodness-of-fit of model to systematic errors. Maximum A-effects differ significantly among subjects, ranging from 21° for FW, to 50° for JG. Subject DB shows a-typical behavior, with small errors at even the largest tilt angles.

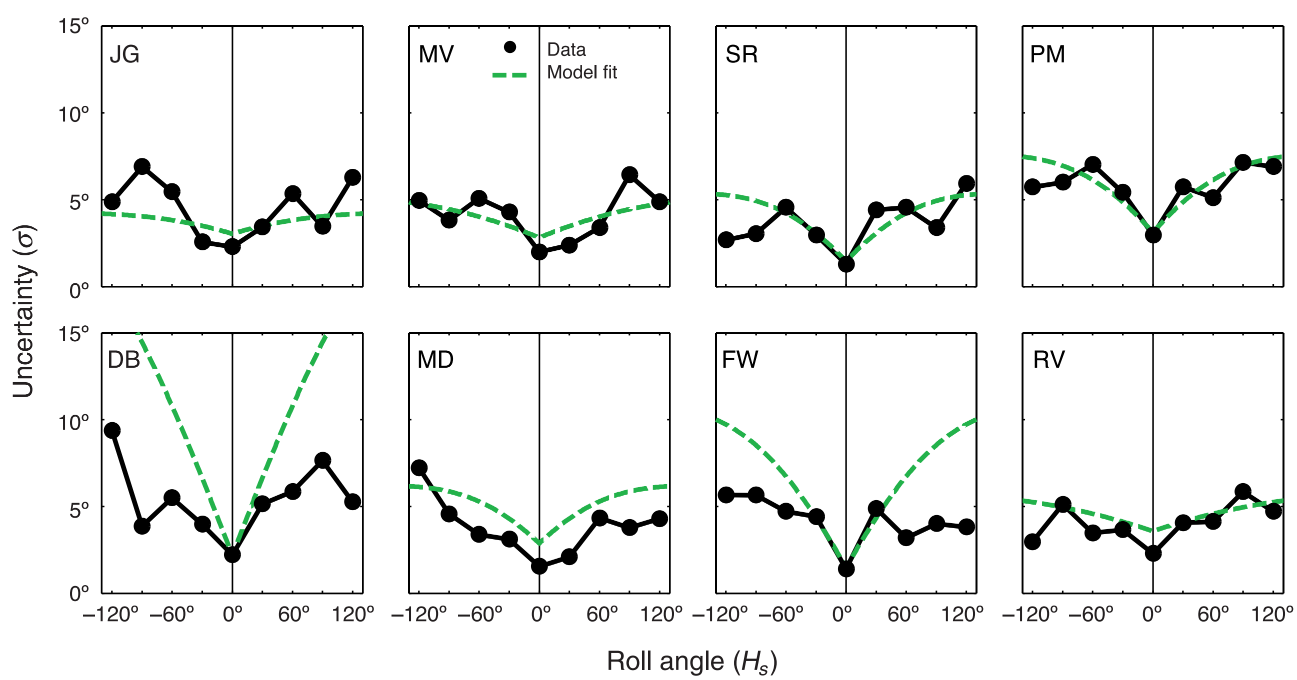

Figure 5. Uncertainty levels (σ) in the SVV task plotted vs. head tilt angle for all subjects. Black circles: σ-values from psychometric functions (see Figure 3). Dashed lines: model fits. For all subjects, σ increases with tilt angle, indicating a decline of precision. Model fits show a modest trend of overestimating σ in most subjects. In subjects FW and DB, overestimation is considerable at large tilts (see main text for explanation).

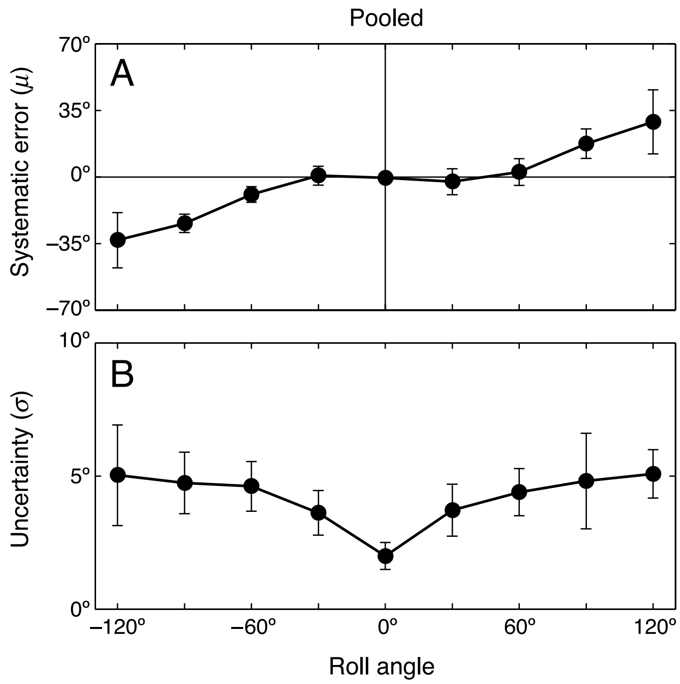

Figure 6. Pooled results from SVV task. (A) Systematic errors, based on μ values ±*SD*. (B) Uncertainty, based on σ values ±*SD* vs. head tilt angle, averaged across subjects.

which is then followed by more gradual increments, resulting in the highest σ values at ±120° roll tilt.

Model fit results

To test whether our model could account for the results, we fitted the model to the data from each subject (see Methods). Note that systematic errors and σ levels, which are coupled in the Bayesian model, were fitted simultaneously. Figure 4 illustrates the fit results of the Bayesian model (dashed lines) in terms of the systematic errors in the SVV. For most subjects, the model fits the systematic error data quite accurately, with R^2-values ≥0.80. Due to the fact that DB has a very unusual error pattern, with only small negative errors at even the largest tilt angles, this fit is considerably worse ($R^2 < 0$)[2]. Note that R^2-values are provided merely to show how well the model accounts for the systematic errors, but do not reflect the overall goodness-of-fit, since σ-levels are equally important. Since the Bayesian model attributes systematic SVV errors to a combination of errors in the head-in-space estimate (A-effects) and in the eye-in-head estimate (E-effects), see Equation 5, we also depicted these opposite contributions separately (red and blue line, respectively). In the three subjects without E-effects (JG, MV, and RV), eye-in-head errors are absent (i.e. $\Delta E_H = 0°$), as illustrated by the blue lines through the abscissa (0°). For the other subjects, the fits indicate the degree of undercompensation for ocular counterroll, reflected by the sinusoidal function. Additional fits of a reduced model that lacked uncompensated ocular counterroll, showed that model fits of JG, MV, and RV did not change. The fits of the five subjects with E-effects worsened significantly (likelihood ratio test, $P \ll 0.01$) and parameter a_0 became unrealistically small (0°). Precision fits, shown in Figure 5, are equally relevant for a complete evaluation of the model. In most subjects (except DB and FW), model fits and actual data show the same trends. Fits show an increase of σ_{SVV} with tilt angle, which is similar to the actual increase observed in the data. Responses from subject DB were rather atypical, also in repeated testing, and therefore difficult to interpret. The overestimation of σ_{SVV} in subject FW appears related to the fact that the systematic error pattern shows increased accuracy at the most negative tilt angle ($H_S = -120°$, see Figure 4). The model has no solution to account for this observation other than by increasing the value of σ_{SVV}. We confirmed this by performing separate fits at positive and negative tilts for subject FW. This resulted in minor differences with regard to the accuracy fits, but strongly affected precision levels: at negative tilts, σ_{SVV} levels were still overestimated, but at positive tilts, the fit improved greatly. This example illustrates how overestimation of σ_{SVV} may be directly related to small discrepancies in the systematic errors of model and data. Moreover, small asymmetries that are present in each observer (see e.g. the *CW*-shift of subject FW in Figure 3) may also affect the fits, because the present model cannot account for such asymmetry. A possible solution would be to allow a shift of the prior on head-in-space, which could be interpreted as a shift in the internal reference frame of the observer.

Best-fit parameter values and associated *SD* levels are listed in Table 2. The best-fit values of parameter a_1 are positive in all subjects (0.03–0.15°/°), which means that noise in the tilt sensors must increase with head-tilt angle if the model is to account for the SVV data. Values of a_0 (mean ±*SD* = 2.8 ± 0.9°), reflecting the sensory head-tilt noise in the upright subject, range from 1.5° for subjects SR and FW, to 4.0° for RV. The width of the head-in-space prior distribution (σ_{Hs}) ranges from 8.5° for subject JG to 21.5° for subject FW (the fit of subject DB reached the arbitrarily chosen limit value). This result indicates that prior knowledge about head tilt has a stronger influence in subject JG than in subject FW. The effect of the width of the head-in-space prior (σ_{Hs}) is best illustrated by comparing subjects JG and MV, where this is the only strikingly different parameter. The prior is narrower in JG than in MV (8.5° vs. 10.5°), which explains why his A-effects are larger. The amplitude of uncompensated eye counterroll (ΔE_H) is significantly larger than zero for the five subjects in which we observed E-effects (SR, PM, DB, MD, and FW). This parameter, which accounts for systematic errors of tilt overcompensation (E-effects), ranges from 8.9° for subject SR to 16.2° for subject MD. In the other three subjects, ΔE_H was zero due to the absence of any E-effects, as shown by Figure 4.

	a_0 [°]	a_1 [°/°]	σ_{H_s}	ΔE_H [°]
JG	3.6 ± 1.1	0.03 ± 0.01	8.5 ± 1.0	0 ± n/a*
MV	3.1 ± 0.4	0.03 ± 0.01	10.5 ± 1.0	0 ± n/a*
SR	1.5 ± 0.4	0.06 ± 0.02	10.7 ± 2.4	8.9 ± 2.7
PM	3.3 ± 1.2	0.08 ± 0.02	15.1 ± 1.9	10.6 ± 2.7
DB	2.2 ± 0.9	0.15 ± 0.03	50.0 ± 1.5	5.8 ± 2.8
MD	3.0 ± 0.8	0.07 ± 0.02	12.3 ± 2.6	16.2 ± 3.4
FW	1.5 ± 0.8	0.10 ± 0.03	21.5 ± 4.7	8.9 ± 2.1
RV	4.0 ± 0.7	0.03 ± 0.01	11.7 ± 1.6	0 ± n/a*

Table 2. Best-fit parameter values (±*SD*) of the SVV data fit. Abbreviations: a_0, noise level $\hat{H}_S$ ($\sigma_{\hat{H}_s}$) at upright; a_1, increase in $\sigma_{\hat{H}_s}$ with tilt angle; σ_{Hs}, width of head prior distribution; ΔE_H, uncompensated eye torsion (see Equation 6). Imposed fit limits, a_0: 0–50°, a_1: 0–3°/°, σ_{Hs}: 0–50°, ΔE_H: 0–20°. *No *SD*-values are available for cases where bootstrapped values formed a skewed distribution.

A further evaluation of parameter variations among all subjects would be contentious, since parameters a_0, a_1, and σ_{Hs} have a combined effect on the systematic errors and uncertainty levels and thus cannot be compared in isolation.

Discussion

Main findings

We investigated the accuracy and precision of the subjective visual vertical (SVV) at nine roll tilt angles in eight subjects, using a psychometric approach. In line with previous studies (Kaptein & Van Gisbergen, 2004; Mittelstaedt, 1983; Van Beuzekom & Van Gisbergen, 2000), we found that SVV accuracy was best at small tilt angles, but decreased at large tilts by showing errors of tilt undercompensation (A-effects). In some subjects, we also observed small but systematic errors of overcompensation (E-effects) at intermediate tilts. Likewise, SVV precision was best at upright (0° head tilt) and deteriorated at larger tilt angles. We fitted a Bayesian model to the set of combined accuracy and precision data, to test the hypothesis that the systematic errors of undercompensation at larger tilts reflect the downside of a strategy to improve precision of the central head-tilt signal at small tilt angles. Similarly, E-effects are interpreted as the side effect of a Bayesian strategy to reduce uncertainty in the estimate of ocular counterroll.

Evaluation of the Bayesian model

Visual signals in the brain are initially encoded in an eye-centered (retinal) frame of reference. To obtain a world-centered percept of visual orientation when the retina's vertical meridian is not aligned with gravity, the brain must convert the original visual signal from retinal to spatial coordinates, using information about eye tilt in space. As early as the 19th century, Aubert already discovered that this transformation is not performed flawlessly (Aubert, 1861). He noticed that subjects who roll-tilted their heads to substantial angles in total darkness, misjudged the world-centered orientation of a visual line, as if they undercompensated for head tilt angle (Aubert or A-effect). Since then, the SVV has been subject of many studies, which confirmed the A-effect at tilt angles >60° and regularly found opposite errors (E-effect) at smaller tilts (Daddaoua, Dicke, & Thier, 2008; Kaptein & Van Gisbergen, 2004; Mittelstaedt, 1983; Schöne, 1964; Udo de Haes, 1970; Van Beuzekom & Van Gisbergen, 2000). Mittelstaedt (1983) was the first to interpret systematic errors in the SVV as the downside of a computational strategy. He hypothesized that the raw head-tilt signal is distorted due to an unequal number of hair cells in the two otolith organs, utricle and saccule. In his model, the brain compensates for these errors by adding a head-fixed idiotropic vector to the biased otolith-based gravity vector. As a result, this strategy reduces errors at small tilts but increases errors at large tilts. More specifically, in Mittelstaedt's model, the E-effect is a remnant of the tilt-signal distortion at modest tilt angles whereas the A-effect at larger tilts partly reflects the additional error induced by the idiotropic vector. Later, Eggert (1998) reformulated Mittelstaedt's model in Bayesian terms and showed that the role of the idiotropic vector was mathematically similar to the role of a head prior in the Bayesian framework. Compared with Eggert's model, the present Bayesian scheme makes different assumptions and proposes a generalized strategy to account for both A- and E-effects. The basic assumption is that the sensory signals concerning head tilt and ocular torsion are veridical, on average, but noisy. This assumption is partly based on the fact that head tilt estimates do not show clear signs of distortion (Mast & Jarchow, 1996; Van Beuzekom et al., 2001) but are corrupted by noise which, if used directly, would lead to high SVV variability. By implementing a generalization of previous schemes (De Vrijer et al., 2008; Eggert, 1998; MacNeilage et al., 2007) the present model reduces noise propagation into the spatial vision stage by relying on knowledge about which head tilt and which eye position are most likely on an *a priori* basis, thereby providing a unified explanation of both A- and E-effects.

Explanation of systematic errors

In the present Bayesian model, the SVV is determined by combining retinal information and information about the orientation of the eyes in space. Computing the eye-in-space estimate involves two stages: estimation of head tilt and estimation of eye-in-head orientation, each incorporating the associated prior knowledge. Whereas the head tilt prior has the beneficial effect of increasing precision of the sensory head tilt estimate, it also causes undercompensation for head tilt, which accounts for A-effects. Likewise, prior knowledge on ocular torsion increases precision in the sensory estimate of ocular torsion, but results in an undercompensation for eye-in-head counterroll and thus leads to an E-effect. Hence, the model accounts for the two types of systematic errors in the SVV by invoking two independent computational stages in the reconstruction of the eye-in-space signal that operate independently and cause opposite bias effects (cf. de Graaf et al., 1992). It can be shown that merging the two stages, using only a single prior for eye in space—relying on an *a priori* assumption that the eyes are generally nearly aligned with gravity—would only explain A-effects.

Once the internal eye-in-space signal is obtained, the model simply adds this signal to the retinal signal. If this linear addition assumption is correct, systematic errors in earth-centric vision should only depend on the tilt angle of the observer, independent on the retinal line orientation used for testing. Findings from two studies (Van Beuzekom et al., 2001; Vingerhoets, Medendorp, & Van Gisbergen, 2008) confirm this prediction. Both studies found that earth-centric estimates of many different line orientations were all subject to virtually the same bias, the magnitude of which depended only on the body tilt angle. This previous work indicates that, apart from a limited degree of distortion (Betts & Curthoys, 1998; Van Beuzekom & Van Gisbergen, 2000), visual space in a tilted observer is virtually uniformly rotated. These findings support the simple linear addition stage and argue against an important role for complex visual–nonvisual interactions or for purely visual phenomena, like the oblique effect (Luyat, Gentaz, Corte, & Guerraz, 2001; Westheimer, 2003).

Is the proposed link between E-effects and ocular counterroll plausible?

Conclusions from previous studies investigating the relation between visual perception and ocular counterroll (OCR) range roughly between two extremes:

1. OCR is not taken into account in spatial perception or
2. the brain perfectly compensates for the effects of OCR.

Wade and Curthoys (1997) argued for the first possibility by showing that the difference between the visual and the manually indicated haptic horizontal (the latter supposedly unaffected by ocular torsion) is closely related to the presence of ocular torsion during visual testing ($r > 0.85$), with slopes varying between 0.57 and 1.51. A further experiment, rotating upright subjects in yaw (Goonetilleke, Mezey, Burgess, & Curthoys, 2008), which induces ocular counterroll but no tilt perception, also revealed a clear correlation between ocular torsion and visual verticality perception (r between 0.4 and 0.8). However, the slope was not unitary, indicating that there was some level of compensation by the visual system. Pavlou, Wijnberg, Faldon, and Bronstein (2003) performing a similar experiment, found clear effects on the SVV, suggesting that approximately 76% of the torsional eye position change was uncompensated and thus affected the SVV. A similar observation was made by de Graaf et al. (1992) in roll-tilted subjects, but only in subjects with persistent E-effects. However, conclusions by Mast (2000) point in a different direction. In this study, SVV results were found to dissociate from ocular torsional changes induced by centrifugation or barbecue rotation. The Bayesian model provides a rational explanation for the variable results of these previous studies, by suggesting the possibility that OCR may only be *partially* taken into account during visual verticality perception.

Since the model fits merely specify the amount of uncompensated ocular counterroll, we could not determine whether a subject with $\Delta E_H = 5°$, for example, had an OCR amplitude of 10° and 50% compensation, or an amplitude of 5° and 0% compensation. All we can do is to regard ΔE_H as the *minimum* OCR amplitude. This implies that, according to the model, the eyes of subject MD counterrolled by at least 16.5°, whereas JG, MV, and RV may not have had any OCR at all (which is rather improbable). Clearly, direct measurements of ocular counterroll in our study would have helped in clarifying this issue, but these were beyond the scope of the study. Another possibility is that the subjects without E-effects had quite normal OCR amplitudes, but compensated perfectly. In the literature, various peak amplitudes of ocular counterroll during static and very slow (quasi-static) tilts have been reported. Population averages roughly vary between 6 and 10° in normal subjects (Diamond & Markham, 1983; Diamond, Markham, Simpson, & Curthoys, 1979; Kingma, Stegeman, & Vogels, 1997; Palla et al., 2006). However, most studies also reported large differences among subjects and Diamond and Markham even found an amplitude range of 2 to 20 degrees during slow (3°/s) dynamic tilts (Diamond and Markham, personal communication, June 11, 2008). Whether the high inter-subject variability in OCR explains the equally variable E-effect, can only be assessed by simultaneous measurement of both variables.

Effect of simplifying assumptions

The question arises to what extent the fit results may have been affected by the fact that visual noise and noise in the eye-torsion estimate were not fitted separately. As a result, in the fits, the parameters representing head-in-space noise and head-tilt prior width (a_0, a_1, σ_{Hs}) also partially reflected the contributions of these additional noise sources (see Methods). We performed several simulations with the Bayesian model to test how large these effects may have been in a worst-case scenario. To do so, we created data through forward simulations of the complete Bayesian model (without simplifications) using the best-fit parameter values of a single subject (PM, see Table 2) combined with a set of values for visual noise ($\sigma_{\hat{L}_E}$), eye-in-head noise (σ_{E_H}) and eye-in-head prior width ($\sigma_{\hat{E}_H}$). The simulated data sets were then fitted with the simplified model, resulting in new parameter values, which were compared with the 'real' values. Even when large values for eye-in-head noise and eye-in-head prior width were used (both 8°) and visual noise was 1°, we found only a slight change in best-fit parameter values. Not surprisingly, parameter a_0, reflecting the offset of tilt noise, was affected most (changing from 3.3 to 6.5°), whereas the other parameters showed only minor changes. We conclude that these simplifying assumptions (see Methods section SVV precision) were warranted and that conclusions remain unchanged.

Evidence for precision-accuracy trade-off in earth-centric vision

Why would the brain apply a strategy that gives rise to systematic errors if the involved sensory signals are all accurate? The answer to this question may be found in the relative precision levels of the sensory systems that are involved in spatial vision. Table 3 gives an overview of the precision levels of the SVV and its underlying signals, as suggested by previous experimental data and the present study.

The visual system is known to be very precise, with just-noticeable-difference (JND) levels for orientation discrimination of maximally 1° for the line length used in our study (Vandenbussche, Vogels, & Orban, 1986). Since the SVV task requires additional sensory information about the spatial orientation of the eyes, SVV precision is worse than in a simple orientation discrimination task and deteriorates with head tilt angle, with average *SD* values of 2.0° at upright and 5.0° at 90° tilt. Can this tilt dependency and the overall decrease of precision be ascribed to the precision characteristics of the compensatory head-tilt and eye-torsion signals? A measure for the precision of the head-tilt signal comes from a study by Mast and Jarchow (1996), who tested subjective body tilt (SBT) in human subjects and found that the average *SD* of body tilt settings was 10.5 ± 3.4° at 90° body tilt. Unpublished psychometric SBT data from our laboratory show a somewhat lower average *SD* level of ~8° at 90° body tilt and an *SD* of ~4.5° near upright. It is interesting to compare these experimental data with the head-tilt noise fit results derived from the present experiments. As can be seen by comparing rows 3 and 4 in Table 3, the model prediction based on the population averaged parameters a_0 and a_1, amounting to an increase from 2.8° at upright to 7.7° at 90° tilt, shows the same trend as the experimentally obtained values in perceived body-tilt experiments. Taken together with the scatter fits in Figure 5, these findings strongly support the model assumption (Equation 2) that noise in the head tilt signal increases with tilt angle. Other studies provide indirect support for this notion. For example, the perturbing effect of roll-optokinetic stimulation on the SVV (Dichgans, Diener, & Brandt, 1974) and on body tilt estimates (Young, Oman, & Dichgans, 1975) becomes more pronounced at larger tilt angles. Similarly, after prolonged roll rotations, the SVV is more strongly affected by residual semicircular canal signals at larger tilt angles (Lorincz & Hess, 2008). Diamond and Markham (1983) showed that variability in OCR, which is thought to be mediated by the utricles (Suzuki, Tokumasu, & Goto, 1969), increases with tilt angle during dynamic tilting. Likewise, Tarnutzer, Bockisch, and Straumann (2007) observed that both SVV and OCR variability increased with tilt angle.

Given that the Bayesian strategy that we propose is geared at reducing noise in the SVV, it is sensible to ask how much noise reduction is actually achieved compared with the scenario of straightforward noise propagation in the contributing signals. Table 3 lists experimentally determined noise levels of the visual signal and the head tilt signal, but none of the internal estimate of eye torsion, since such data are (understandably) not available. Even if we ignore the contribution of eye-torsion noise in a noise propagation scenario, simple computations show that precision levels in visual spatial perception would be quite poor (4.6° at 0° tilt and 10.5° at 90° tilt) based on these three sensory signals in a straightforward manner. The fact that the actual SVV precision is so much better

Signal		0° tilt	90° tilt	Evidence	References
Visual, measured	($\sigma_{\hat{L}_E}$)	1°	1°	data	Vandenbussche et al., 1986
SVV, measured	(σ_{SVV})	2.0 ± 0.6°	5.0 ± 1.5°	data	present study
SBT, measured	(σ_{SBT})	4.5 ± 1.0°	10.5 ± 3.4°	data	0° tilt: unpublished own data 90° tilt: Mast and Jarchow, 1996
SBT, predicted	($\sigma_{\hat{H}_S}$)	2.8 ± 0.9°	7.7 ± 1.9°	fit result	present study

Table 3. Precision levels of signals involved in spatial vision. Abbreviations: SVV = subjective visual vertical, SBT = subjective body tilt. SBT precision is assumed to reflect the precision of the sensory head-tilt signal ($\sigma_{\hat{H}_S}$). The 0° tilt value (3rd row) is based on unpublished psychometric data from our laboratory. Predicted SBT precision values (4th row) directly result from average best-fit parameter values of a_0 and a_1 (see Table 2).

can now be understood as being the result of a precision-accuracy trade-off based on a Bayesian strategy that aims at high precision, at the cost of reduced accuracy.

Appendix A

Bayesian model: Derivation of Equations 3 and 4

In case of a single trial, the optimal estimate of head tilt angle ($\tilde{H}_S$), for given sensory signal $\hat{H}_S$ and prior information, is obtained by applying Bayes' rule, and is defined by:

$$\tilde{H}_S = \frac{\sigma^2_{H_S}}{\sigma^2_{H_S} + \sigma^2_{\hat{H}_S}} \cdot \hat{H}_S \tag{A1}$$

This relation is obtained by taking the maximum value of the posterior distribution. The expected value (μ) of $\tilde{H}_S$ in many repeated trials is then specified by:

$$\mu_{\tilde{H}_S} = \frac{\sigma^2_{H_S}}{\sigma^2_{H_S} + \sigma^2_{\hat{H}_S}} \cdot \mu_{\hat{H}_S} = \frac{\sigma^2_{H_S}}{\sigma^2_{H_S} + \sigma^2_{\hat{H}_S}} \cdot H_S \tag{A2}$$

which equals the first term of Equation 3. The variance of $\hat{H}_S$ determines the variance of $\tilde{H}_S$ according to:

$$\mathrm{var}\left(\tilde{H}_S\right) = \left(\frac{\partial \tilde{H}_S}{\partial \hat{H}_S}\right)^2 \cdot \mathrm{var}\left(\hat{H}_S\right) = \left(\frac{\sigma^2_{H_S}}{\sigma^2_{H_S} + \sigma^2_{\hat{H}_S}}\right)^2 \cdot \sigma^2_{\hat{H}_S} \tag{A3}$$

which is equivalent to the first term of Equation 4. The same principle applies to the mean value and variance of the eye-in-head estimate ($\tilde{E}_H$):

$$\mu_{\tilde{E}_S} = \frac{\sigma^2_{E_H}}{\sigma^2_{E_H} + \sigma^2_{\hat{E}_H}} \cdot \mu_{\hat{E}_H} = \frac{\sigma^2_{E_H}}{\sigma^2_{E_H} + \sigma^2_{\hat{E}_H}} \cdot A\sin(H_S) \tag{A4}$$

which equals the second term of Equation 3. Here we use the assumption that the expected value of $\hat{H}_S$ is equal to the real head-in-space angle (H_S). For the variance in the eye-in-head estimate we deduce,

$$\mathrm{var}\left(\tilde{E}_H\right) = \left(\frac{\partial \tilde{E}_H}{\partial \hat{E}_H}\right)^2 \cdot \mathrm{var}\left(\hat{E}_H\right) = \left(\frac{\sigma^2_{E_H}}{\sigma^2_{E_H} + \sigma^2_{\hat{E}_H}}\right)^2 \cdot \sigma^2_{\hat{E}_H} \tag{A5}$$

which is equal to the second term of Equation 5.

Acknowledgments

We thank H. Kleijnen, G. van Lingen, S. Martens, and G. Windau for technical support. This work was supported by Donders Centre for Cognition and Faculteit der Natuurwetenschappen, Wiskunde en Informatica of Radboud University Nijmegen and by grants from the Netherlands Organization for Scientific Research and the Human Frontier Science Program to W. P. Medendorp.

Commercial relationships: none.
Corresponding author: Maaike De Vrijer.
Email: m.devrijer@donders.ru.nl.
Address: Donders Institute for Brain, Cognition and Behaviour, Radboud University Nijmegen, PO Box 9101, 6500 HB Nijmegen, The Netherlands.

Footnotes

[1]The term *accuracy* refers to constant errors (bias) in the response. Precision is linked to variable errors, which reflect noise in the system (Howard, 1982).

[2]R^2 reflects the amount of variance in the data that is explained by the fit and is not really a squared value. Here, an R^2-value < 0 means that a straight line would fit the data better than the Bayesian model fit.

References

Aubert, H. (1861). Eine scheinbare Drehung von Objekten bei Neigung des Kopfes nach rechts oder links. *Virchows Archiv: Official Journal of the European Society of Pathology, 20,* 381–393.

Betts, G. A., & Curthoys, I. S. (1998). Visually perceived vertical and visually perceived horizontal are not orthogonal. *Vision Research, 38,* 1989–1999. [PubMed]

Carandini, M. (2006). Measuring the brain's assumptions. *Nature Neuroscience, 9,* 468–470. [PubMed]

Curthoys, I. S. (1996). The role of ocular torsion in visual measures of vestibular function. *Brain Research Bulletin, 40,* 399–403. [PubMed]

Daddaoua, N., Dicke, P. W., & Thier, P. (2008). The subjective visual vertical in a nonhuman primate. *Journal of Vision, 8*(3):19, 1–8, http://journalofvision.org/8/3/19/, doi:10.1167/8.3.19. [PubMed] [Article]

de Graaf, B., Bekkering, H., Erasmus, C., & Bles, W. (1992). Influence of visual, vestibular, cervical, and somatosensory tilt information on ocular rotation and perception of the horizontal. *Journal of Vestibular Research, 2,* 15–30. [PubMed]

De Vrijer, M., Medendorp, W. P., & Van Gisbergen, J. A. (2008). Shared computational mechanism for tilt compensation accounts for biased verticality percepts in motion and pattern vision. *Journal of Neurophysiology, 99,* 915–930. [PubMed]

Diamond, S. G., & Markham, C. H. (1983). Ocular counterrolling as an indicator of vestibular otolith function. *Neurology, 33,* 1460–1469. [PubMed]

Diamond, S. G., Markham, C. H., Simpson, N. E., & Curthoys, I. S. (1979). Binocular counterrolling in humans during dynamic rotation. *Acta Oto-Laryngologica, 87,* 490–498. [PubMed]

Dichgans, J., Diener, H. C., & Brandt, T. (1974). Optokinetic-graviceptive interaction in different head positions. *Acta Oto-Laryngologica, 78,* 391–398. [PubMed]

Dyde, R. T., Jenkin, M. R., & Harris, L. R. (2006). The subjective visual vertical and the perceptual upright. *Experimental Brain Research, 173,* 612–622. [PubMed] [Article]

Eggert, T. (1998). *Der Einfluss orientierter Texturen auf die subjektive visuelle Vertikale und seine systemtheoretische Analyse (PhD Thesis)*. Munich Technical University, Munich, Germany.

Ehrenstein, W. H., & Ehrenstein, A. (1999). Psychophysical methods. In U. Windhorst, & H. Johansson (Eds.), *Modern techniques in neuroscience research* (pp. 1211–1241). Berlin: Springer-Verlag.

Goonetilleke, S. C., Mezey, L. E., Burgess, A. M., & Curthoys, I. S. (2008). On the relation between ocular torsion and visual perception of line orientation. *Vision Research, 48,* 1488–1496. [PubMed]

Howard, I. P. (1982). *Human visual orientation*. New York: Wiley.

Kaptein, R. G., & Van Gisbergen, J. A. (2004). Interpretation of a discontinuity in the sense of verticality at large body tilt. *Journal of Neurophysiology, 91,* 2205–2214. [PubMed] [Article]

Kingma, H., Stegeman, P., & Vogels, R. (1997). Ocular torsion induced by static and dynamic visual stimulation and static whole body roll. *European Archives of Oto-Rhino-Laryngology, 254,* S61–S63. [PubMed]

Knill, D. C., & Pouget, A. (2004). The Bayesian brain: The role of uncertainty in neural coding and computation. *Trends in Neurosciences, 27,* 712–719. [PubMed]

Lorincz, E. N., & Hess, B. J. (2008). Dynamic effects on the subjective visual vertical after roll rotation. *Journal of Neurophysiology, 100,* 657–669. [PubMed]

Luyat, M., Gentaz, E., Corte, T. R., & Guerraz, M. (2001). Reference frames and haptic perception of orientation: Body and head tilt effects on the oblique effect. *Perception & Psychophysics, 63,* 541–554. [PubMed]

MacNeilage, P. R., Banks, M. S., Berger, D. R., & Bülthoff, H. H. (2007). A Bayesian model of the disambiguation of gravitoinertial force by visual cues. *Experimental Brain Research, 179,* 263–290. [PubMed] [Article]

Markham, C. H., & Diamond, S. G. (2002). Ocular counterrolling in response to static and dynamic tilting: Implications for human otolith function. *Journal of Vestibular Research, 12,* 127–134. [PubMed]

Mast, F. W. (2000). Does the world rock when the eyes roll? Allocentric orientation representation, ocular counterroll, and the subjective vertical. *Swiss Journal of Psychology, 59,* 89–101.

Mast, F., & Jarchow, T. (1996). Perceived body position and the visual horizontal. *Brain Research Bulletin, 40,* 393–397. [PubMed]

Mittelstaedt, H. (1983). A new solution to the problem of the subjective vertical. *Naturwissenschaften, 70,* 272–281. [PubMed]

Müller, G. E. (1916). Über das Aubertsche Phänomen. *Zeitschrift für Sinnesphysiologie, 49,* 109–246.

Palla, A., Bockisch, C. J., Bergamin, O., & Straumann, D. (2006). Dissociated hysteresis of static ocular counterroll in humans. *Journal of Neurophysiology, 95,* 2222–2232. [PubMed] [Article]

Pavlou, M., Wijnberg, N., Faldon, M. E., & Bronstein, A. M. (2003). Effect of semicircular canal stimulation on the perception of the visual vertical. *Journal of Neurophysiology, 90,* 622–630. [PubMed] [Article]

Schöne, H. (1964). On the role of gravity in human spatial orientation. *Aerospace Medicine* (August), 764–772.

Suzuki, J. I., Tokumasu, K., & Goto, K. (1969). Eye movements from single utricular nerve stimulation in the cat. *Acta Oto-Laryngologica, 68,* 350–362. [PubMed]

Tarnutzer, A. A., Bockisch, C. J., & Straumann, D. (2007). *Variability of subjective visual vertical and ocular counterroll are correlated, Program No. 861.1.* Paper presented at the 37th meeting of the Society for Neuroscience, 2007, San Diego, CA.

Udo de Haes, H. (1970). Stability of apparent vertical and ocular countertorsion as a function of lateral tilt. *Perception and Psychophysics, 8,* 137–142.

Van Beuzekom, A. D., Medendorp, W. P., & Van Gisbergen, J. A. (2001). The subjective vertical and the sense of self orientation during active body tilt. *Vision Research, 41,* 3229–3242. [PubMed]

Van Beuzekom, A. D., & Van Gisbergen, J. A. (2000). Properties of the internal representation of gravity inferred from spatial-direction and body-tilt estimates. *Journal of Neurophysiology, 84,* 11–27. [PubMed] [Article]

Vandenbussche, E., Vogels, R., & Orban, G. A. (1986). Human orientation discrimination: Changes with eccentricity in normal and amblyopic vision. *Investigative Ophthalmology & Visual Science, 27,* 237–245. [PubMed] [Article]

Vingerhoets, R. A., Medendorp, W. P., & Van Gisbergen, J. A. (2008). Body-tilt and visual verticality perception during multiple cycles of roll rotation. *Journal of Neurophysiology, 99,* 2264–2280. [PubMed]

Wade, S. W., & Curthoys, I. S. (1997). The effect of ocular torsional position on perception of the roll-tilt of visual stimuli. *Vision Research, 37,* 1071–1078. [PubMed]

Westheimer, G. (2003). Meridional anisotropy in visual processing: Implications for the neural site of the oblique effect. *Vision Research, 43,* 2281–2289. [PubMed]

Wichmann, F. A., & Hill, N. J. (2001a). The psychometric function: I. Fitting, sampling, and goodness of fit. *Perception & Psychophysics, 63,* 1293–1313. [PubMed]

Wichmann, F. A., & Hill, N. J. (2001b). The psychometric function: II. Bootstrap-based confidence intervals and sampling. *Perception & Psychophysics, 63,* 1314–1329. [PubMed]

Young, L. R., Oman, C. M., & Dichgans, J. M. (1975). Influence of head orientation on visually induced pitch and roll sensation. *Aviation, Space, and Environmental Medicine, 46,* 264–268. [PubMed]